Structural Engineering and Mechanics, Vol. 43, No. 5 (2012) 657-678
DOI: http://dx.doi.org/10.12989/sem.2012.43.5.657

Implementation of a micro-meso approach for progressive damage analysis of composite laminates

H. Hosseini-Toudeshky*[1], A. Farrokhabadi[2a] and B. Mohammadi[3b]

[1]*Department of Aerospace Engineering, Amirkabir University of Technology, No. 424, Hafez Ave., Tehran, Iran*
[2]*Department of Aerospace Engineering, Semnan University, Semnan, Iran*
[3]*School of Mechanical Engineering, Iran University of Science and Technology, Narmak, Tehran, Iran*

(Received February 4, 2012, Revised May 24, 2012, Accepted August 9, 2012)

Abstract. The mismatch of ply orientations in composite laminates can cause high interlaminar stress concentrations near the free edges. Evaluation of these interlaminar stresses and their role in the progressive damage analysis of laminates is desirable. Recently, the authors developed a new method to relate the physically based micromechanics approach with the meso-scale CDM considering matrix cracking and induced delamination. In this paper, the developed method is applied for the analysis of edge effects in various angle-ply laminates such as $[10/-10]_{2s}$, $[30/-30]_{2s}$ and $[45/-45]_{2s}$ and comparing the results with available traditional CDM and experimental results. It is shown that the obtained stress-strain behaviors of laminates are in good agreement with the available experimental results and even in better agreement than the traditional CDM results. Variations of the stresses and stiffness components through the laminate thickness and near the free edges are also computed and compared with the available CDM results.

Keywords: micro-meso; edge effects; progressive damage; continuum damage

1. Introduction

Composite laminates are considerably sensitive to edge effects due to mismatching of material properties of various layers with different orientations. While laminates are primarily designed to withstand in-plane loadings, high interlaminar stresses at free edges, holes and cut-outs can affect the material properties of laminate. This phenomenon could lead to different damage modes including matrix cracking and induced delamination when the applied loading is even lower than the failure strength predicted by classical lamination theory (Nguyen and Caron 2006). Experimental observations show that initiation and propagation of edge delamination are due to the correlation between the matrix crack density and free-edge effects. Several approaches have been proposed for edge effects analysis including finite difference, higher-order plate theory, boundary layer theory, approximate elasticity solutions and finite elements method (Kant and Swaminathan 2000). However, due to the complex nature of damage mechanisms, the problem continues to attract

*Corresponding author, Professor, E-mail: Hosseini@aut.ac.ir
[a]Assistant Professor, E-mail: amin.farrokh@profs.semnan.ac.ir
[b]Assistant Professor, E-mail: Bijan_Mohammadi@iust.ac.ir

research interest.

Continuum damage mechanics (CDM) is one of the most well known and powerful approaches for analyzing the nonlinear damage behavior of materials which has been established and developed in recent years. Many researchers followed the concept of CDM for analyzing various types of damages including microcracks, fiber breakage and interface debonding in composites (Mishnaevsky and Brøndsted 2009). In the initial work using CDM, isotropic damage condition was mainly assumed and the damage parameter was considered as a scalar factor only (Chaboche and Maire 2002). To consider anisotropic damage, the first and second order of damage tensors was proposed. In the subsequent numerical approaches, the four and eighth order damage tensor was also considered (Chaboche and Maire 2002). It is worth to note that by increasing the order of damage tensor, the multiplicity of unknown parameters is increased which should be obtained from standard and nonstandard characterization experiments. Lee *et al*. (1989) applied CDM approach to develop a progressive damage model for the homogenized composite material at the ply level. They considered a second order damage tensor for distributed microscopic damages. The nonlinear response due to both damage and plasticity phenomena were considered by Voyiadjis and Kattan (1999), Voyiadjis and Park (1999), Voyiadjis and Deliktas (2000), Voyiadjis *et al.* (2001) in the framework of CDM. They developed a 3D model using a symmetric second order damage tensor in which the microcrack density was obtained from the eigen-values of the damage tensor. Voyiadjis and Deliktas (2000) proposed a micromechanical based approach for considering both damage and plastic deformations into the analysis of metal matrix composite materials. They characterized three damage modes including matrix damage, fiber damage and interfacial debonding. Barbero and DeVivo (2001) applied a symmetric second order damage tensor in CDM framework for modeling the progressive damage analysis of composite laminates. For this purpose, they developed a two-dimensional (2D) plane stress model in which damage evolution and stiffness reduction were computed for the pre-homogenized composite material simplifying the formulation. Villiam *et al*. (2003) proposed a two dimensional CDM approach for composite laminate using shell elements and applied their model in an explicit nonlinear FEM code. Abu Al-Rub and Voyiadjis (2003) developed their CDM model to consider different interaction mechanisms between damage and plasticity defects using two-isotropic and two kinematic hardening evolution laws. Also an additive decomposition of the total strain into elastic, plastic, and damage parts was proposed in their work. Lonetti *et al*. (2003) performed further development on Barbero's model to include tri-axial orthotropic damage in terms of three damage eigenvalues. They used a tri-axial damage model in the 3D solid finite element methods. Raghavan and Ghosh (2005) developed a CDM model for composite laminate and used interface element for simulating the cohesive zone model. They determined the damage parameter and damage flow rule using the micromechanical analysis of a representative unit cell. Camanho *et al*. (2007) established a two dimension thermodynamic model to simulate the damage evolution of composite laminates by relating the CDM theory with the finite element method. Liu and Zhang (2008) proposed an energy-based CDM model to predict the progressive failure properties of cylindrical composite laminates. They considered three failure modes including fiber breakage, matrix cracking and fiber/matrix interface shear failure and three damage evolution laws include different damage variables and conjugate forces proposed. Varna (2008) developed a CDM model and used a theoretical framework to link the macro response of a damaged laminate to the opening and sliding displacements of crack surfaces in an exact form. By this way he could generate second order damage tensors related to crack face opening and sliding. Hassan and Batra (2008) used CDM approach with three scalar damage variables related to fiber failure, matrix cracking and interface debonding and modeled the damage evolution in polymeric composites. Mohammadi *et al*. (2008, 2009) investigated the progressive damage and overall response of composite laminates under quasi-static monotonic in-plane loading using three-dimensional CDM theory implemented in a finite element layer-wise method. Falzon and Apruzzese (2011) developed a 3D continuum damage mechanics-based material model which employed in an implicit FE code to simulate the progressive intralaminar degradation of fibre reinforced laminates. They considered seven damage parameters assigned to tensile, compressive and shear damage at a ply level.

In the classical CDM, the damage tensor describes the general behavior of damage mechanisms without distinction of individual damage modes. Ladeveze *et al*. (2000), proposed a new approach using continuum damage mechanics in the meso-scale. The main concept of this meso modeling was the definition of particular scalar damage parameters related to each damage mode that are incident in laminated composites. On this intermediary scale, the material was described by means of two basic meso-constituents of the single layer and interface. Thus, the laminated structure was described as a stacking sequence of homogeneous layers throughout the thickness and interlaminar interfaces (Ladeveze *et al*. 2000). For both of the two basic constituents, i.e., the ply and the interface, material models were introduced using the internal variables framework for specifying the state of material. The meso damage indicators are linked to the stiffness variation of the meso constituents. The advantage of this procedure is that damage mechanisms, which can be very complex on the structure's scale, could be quite simple on the scale of basic constituents (Ladeveze *et al*. 2000). Further, Ladeveze *et al*. (2006) tried to extend their proposed approach to out-of-plane macro loading in order to deal with delamination. Mesomechanics models are capable of predicting different damage mechanisms and their evolution until final failure. In addition, these models are applicable to industrial structures subjected to complex loading, providing a general formulation, and can be more easily integrated into commercial software. One of the major differences between the developed CDM in meso scale by Ladeveze and classical CDM approach is using the non-associated flow rule in meso scale. Thus, this approach requires additional empirical constants and needs specific tests for each layup that are necessary to obtain the non-associated flow rule parameters in damage condition.

Recently, the authors of this paper developed a micro-meso approach in the framework of CDM benefited from both strong physical meaning of micromechanics and capability of mesomechanics approaches (Farrokhabadi *et al*. 2010, 2011, In Press). It is worth to note that in the previously developed classical CDM approaches and CDM in meso scale, the damage evolution law and its related material data are obtained by numerous layup dependent standard and nonstandard experiments, which are costly and time consuming. The major novelty of our proposed methodology is using the concept of micromechanics inside the mesomechanics approach to obtain the damage parameters and relation between the conjugate forces and damage parameters. Whereas in the developed mesomechanics model by Ladeveze *et al*. (2000), these parameters are obtained from different experiments, the proposed micro-meso approach improved this major disadvantage which is the requirement of specific tests for various layups to obtain the non-associated flow rule parameters in damage conditions.

In this paper, the capability of the developed micro-meso approach in the framework of CDM for the analyses of laminates prone to edge effects is examined. For this purpose, the developed code is used for consideration of edge effects in progressive damage analyses and final failure load prediction of various angle-ply laminates under monotonic loading. The obtained results are compared with the available experimental and CDM results.

2. Generic procedure statement

The major key point for considering damage progress in laminated composites is modeling of damage growth in each layer separately and independent of other layers using the appropriate evolution laws. To obtain the conjugate forces and damage parameters of meso model from the micromechanics approach, a single orthotropic composite lamina under a general stress field should be considered which is prone to matrix cracking and induced delamination. Following that, the micromechanics approach is used to derive the governing relations for stress and displacement fields at a specific crack density or delamination length. Contrary to the previous approaches, in the presented micromechanics method by the authors, the relations are obtained for a single lamina unit cell under multi-axial loading conditions (Farrokhabadi *et al*. 2010, In Press). The full explanations of the method were presented in Farrokhabadi *et al*. (2010, 2011, In Press). Using the explained micromechanics formulations along with the concept of continuum damage mechanics it is possible to define the damage parameters related to each damage mode that shows the stiffness degradation of the single lamina due to the considered damage modes (Farrokhabadi *et al*. 2010, 2011). These parameters were employed in the mesomechanics approach to establish a new micro-meso approach, which can be used to predict the nonlinear response and progressive damage of different composite laminates due to the matrix cracking and induced delamination growth without limitation in layup configuration and under multi axial stress conditions.

3. Theoretical modeling of elementary ply

To consider the elementary ply in meso modeling a single lamina under general normal and shear stresses on all edges is considered which is prone to matrix cracking and induced delamination. For precise behavior modeling, the tri-axial deformation of orthotropic composite lamina is considered. For this elementary ply, three damage parameters related to its probable damage modes are considered which can affect the stiffness matrix and strain energy of single lamina after damage formation as follow

$$\tilde{C} = \begin{bmatrix} \frac{1}{E_x} & \frac{-\upsilon_{xy}}{E_x} & \frac{-\upsilon_{xz}}{E_x} & 0 & 0 & 0 \\ \frac{-\upsilon_{xy}}{E_x} & \frac{1}{E_y(1-d_2)} & \frac{-\nu_{yz}}{E_y(1-d_2)} & 0 & 0 & 0 \\ \frac{-\upsilon_{xz}}{E_x} & \frac{-\nu_{yz}}{E_y(1-d_2)} & \frac{1}{E_z(1-d'')} & 0 & 0 & 0 \\ 0 & 0 & 0 & \frac{1}{G_{xy}(1-d')} & 0 & 0 \\ 0 & 0 & 0 & 0 & \frac{1}{G_{xz}(1-d'')} & 0 \\ 0 & 0 & 0 & 0 & 0 & \frac{1}{G_{xy}(1-d')} \end{bmatrix} \tag{1}$$

In the obtained stiffness matrix of $\tilde{C}$, three scalar damage parameters of d_2, d' and d'' are considered. The damage parameter of d_2 affects the in-plane transverse direction property of material coordinate system, E_y. Also, the damage parameter of d', affects the in-plane shear modulus of G_{xy} and damage parameter of d'' remarks the out of plane shear modulus of G_{xz} and E_z. The major key point in the meso-modeling is to obtain theses damage parameters and their evolution law.

Having the stiffness matrix in damage condition, the stress-strain relations and strain energy for the damaged lamina are $\sigma = \tilde{C}\varepsilon$ and $\tilde{E} = \frac{1}{2}\varepsilon\tilde{C}\varepsilon$ respectively. Therefore, the strain energy of damaged single lamina can be obtained as a function of lamina material properties and damaged parameters as follows

$$\tilde{E} = \frac{1}{2}\left(\frac{\sigma_x^2}{E_x} - \frac{\upsilon_{xy}}{E_x}\sigma_x\sigma_y - \frac{\upsilon_{xz}}{E_x}\sigma_x\sigma_z - \frac{\upsilon_{yx}}{E_y(1-d_2)}\sigma_x\sigma_y + \frac{\sigma_y^2}{E_y(1-d_2)} - \frac{\upsilon_{yz}}{E_y(1-d_2)}\sigma_x\sigma_y\right.$$
$$\left. - \frac{\upsilon_{zx}}{E_z(1-d'')}\sigma_x\sigma_z \frac{\upsilon_{yz}}{E_y(1-d_2)}\sigma_y\sigma_z + \frac{\sigma_z^2}{E_z(1-d'')}\right) + \frac{1}{2}\left(\frac{\sigma_{xy}^2}{G_{xy}(1-d')} + \frac{\sigma_{xz}^2}{G_{xz}(1-d'')} + \frac{\sigma_{yz}^2}{G_{yz}(1-d'')}\right)\Bigg) \quad (2)$$

Having the strain energy of damaged single layer, the 'thermodynamic forces, **Y**, or strain energy release rate can be calculated from $Y = \partial\tilde{E}/\partial d$. Now, by definition of strain energy as a function of damage parameters for both damage mechanisms of matrix cracking and induced delamination, the non-associated flow rule (relation between thermodynamic forces and damage parameters) could be developed using separate constitutive relations as well.

4. Definition of specific damage parameter

The important ingredients in mesomechanics approach are definition of damage evolution law and damage parameter for each damage mechanism in any loading condition. In the previously developed mesomechanics approaches, these parameters were defined by numerous standard and nonstandard tests. For example for considering the matrix crack and induced delamination in each layer apart from initial elastic characteristics, the model depends on the material parameters such as Y_c, Y_c', Y_0, Y_0', Y_s', and b, which define the damage-evolution laws (Ladeveze *et al*. 2000). In addition, the relation between the damage parameters and associated forces of Y should be defined by specific loading-unloading tests on special angle ply laminates. In the proposed approach by the authors, a new micromechanics modeling are used to obtain the mentioned damage parameters. As expressed before, for this purpose the micromechanics approach was developed for a single layer which is prone to matrix cracking and induced delamination growth. The micromechanics of single layer was developed by the authors for matrix cracking (2010, In Press) and for matrix cracking and induced delamination (2011). This model has the capability of estimating the stress and displacement fields of damaged single layer under multiaxial loadings. In this method, damage parameters of d_2 and d' were defined for crack density and induced delamination length respectively. For this purpose, the stress-strain relations and ply crack closure for constrained uni-axial loading in axial, transverse and through the thickness directions were used and three independent constants of d_2, d_{21} and d_{23} were obtained which were used for deriving the damaged parameters of single layer. This means that the obtained damage parameters by the considered assumptions consider the closure effects and don't increase in compression loading.

$$d_2 = 1 - \frac{E_y(\rho, \delta)}{E_y}; \quad \frac{\nu_{yx}}{E_y} - \frac{\nu_{yx}(\rho, \delta)}{E_y(\rho)} = \frac{d_{21}d_2}{E_y(1-d_2)}$$

$$\frac{1}{E_x} - \frac{1}{E_x(\rho, \delta)} = \frac{d_{21}^2 d_2}{E_y(1-d_2)}; \quad \frac{\nu_{yz}}{E_y} - \frac{\nu_{yz}(\rho, \delta)}{E_y(\rho, \delta)} = \frac{d_{23}d_2}{E_y(1-d_2)}$$

$$\frac{1}{E_z} - \frac{1}{E_z(\rho, \delta)} = \frac{d_{23}^2 d_2}{E_y(1-d_2)}; \quad \frac{\nu_{xz}}{E_x} - \frac{\nu_{xz}(\rho, \delta)}{E_x(\rho, \delta)} = \frac{d_{21}d_{23}d_2}{E_y(1-d_2)}$$

$$d' = 1 - \frac{G_{xy}(\rho, \delta)}{G_{xy}} \tag{3}$$

It is worth to mention that the damage parameters of d_2 and d' affect the in plane modulus of lamina E_y and G_{xy} only. To consider the effects of damage parameters on the out of plane shear modulus of lamina (G_{xz}) which is important for the edge effects, the third damage parameter of d'' is defined. This damage parameter is defined by the concept of CDM which can be changed proportional to the damage surface. Therefore, this new damage parameter d'' could be evaluated by increasing the induced delamination length as $d'' = l_d/l_{element}$.

5. Definition of damage evolution law

To study the damage growth of laminates using CDM, an appropriate evolution law describing the evolution of damage state is required. In the traditional CDM with meso-scale approaches (ladeveze *et al*. 2000), definition of damage evolution law and its related parameters require numerous standard and non-standard layup dependent tests. However, using the micromechanics approaches, damage evolution can be predicted by comparing the computed strain energy release rate of the damaged unit cell with the finite fracture toughness only which is employed in this study (Farrokhabadi *et al*. 2010). According to this concept, in the developed micromechanics model by the authors (2010, In Press), it is assumed that the matrix cracking evolutions are evenly formed when the strain energy release rate reaches to the finite fracture toughness of matrix cracking (G_{mc}). The strain energy release rate for matrix cracking is calculated by

$$(G_m - G_{mc}) > 0$$

$$G_m = \frac{1}{\Delta A_m}\left(\int \frac{1}{2}\{\sigma(\rho)\}^T[S]\{\sigma(\rho)\}dV - \int \frac{1}{2}\{\sigma\}^T[S]\{\sigma\}dV\right) \tag{4}$$

Where, ΔA_m is the crack surface area due to the matrix crack density, ρ which is defined by the lamina thickness multiplied by the unit cell width. The expressions $\int \frac{1}{2}\{\sigma(\rho)\}^T[S]\{\sigma(\rho)\}dV$ and $\int \frac{1}{2}\{\sigma\}^T[S]\{\sigma\}dV$ define the strain energy for cracked lamina with ρ, crack density, and undamaged lamina respectively.

The sduced delamination initiation and propagation can be also predicted by equating the calculated energy release rate due to delamination formation from the matrix crack tips (G_d) to the respective critical strain energy release rate, (G_{dc}).

$$(G_d - G_{dc}) > 0$$

$$G_d = \frac{1}{\Delta A_d}\left(\int_{\substack{After\\Delam.}} \frac{1}{2}\{\sigma(\rho,\delta)\}^T[S]\{\sigma(\rho,\delta)\}dV - \int_{\substack{Before\\Delam.}} \frac{1}{2}\{\sigma(\rho)\}^T[S]\{\sigma(\rho)\}dV \right) \tag{5}$$

In this equation, ΔA_d is the created crack surface area due to the delamination growth which is defined by delamination length multiply by the unit cell width. The expression of $\int_{\substack{Before\\Delam.}} \frac{1}{2}\{\sigma(\rho)\}^T[S]\{\sigma(\rho)\}dV$ defines the strain energy of the unit cell containing matrix crack before delamination initiation. The expression of $\int_{\substack{After\\Delam.}} \frac{1}{2}\{\sigma(\rho,\delta)\}^T[S]\{\sigma(\rho,\delta)\}dV$ also defines the strain energy of damaged 90º lamina containing both matrix crack and induced delamination. The matrix cracking fracture toughness (G_{mc}) and critical strain energy release rate for delamination (G_{dc}) are determined from experiments.

6. Proposed micro-meso approach

In this section the overall concepts of the developed progressive damage model based on the micro-meso approach are presented. As stated before, the developed micromechanics model by the authors has the capability of analyzing the stress distribution of damaged unit cell, evaluating the strain energy release rates due to each damage mode of matrix crack/induced delamination, determining the related damage parameters and predicting the damage growth using only the fracture toughness of lamina as material damage parameter. These capabilities can be used for determining the damage evolution law and required damage parameters, which are necessary for nonlinear progressive damage analysis of laminates. Defining the damage evolution law in traditional classic mesomechanics approaches needs numerous standard and nonstandard layup tests (Ladeveze *et al*. 2000). In the present study, by combining the micromechanics and mesomechanics approaches simultaneously, a relatively new micro-meso model is proposed to overcome the major disadvantage of traditional meso-scale modeling and it is applicable for composite laminates with general layup configuration.

The explained micro-meso approach were programmed and added to the features of an available CDM code benefited from layer-wise formulation (Mohammadi *et al*. 2008). For this purpose, each layer of each element is decomposed (Fig. 1(a) and (b)) and considered as a unit cell which means that the initial unit cell dimensions are equal to the element sizes (Fig. 1(c)). The remote stress boundaries of considered unit cells are determined from the FE solution of laminates in each load step. Having the boundary stresses of different unit cells at various points of the laminate, it is possible to examine the state of damage growth using the developed micromechanics approach in an extended subroutine.

The dimensions of each unit cell including the unit cell length and its delaminated part are virtually changed by variation of crack density (Fig. 1(d)) or induced delamination evolution (Fig. 1(e)) as shown in Fig. 1(d) and (e). The calculation steps for matrix crack evolution in this subroutine are:

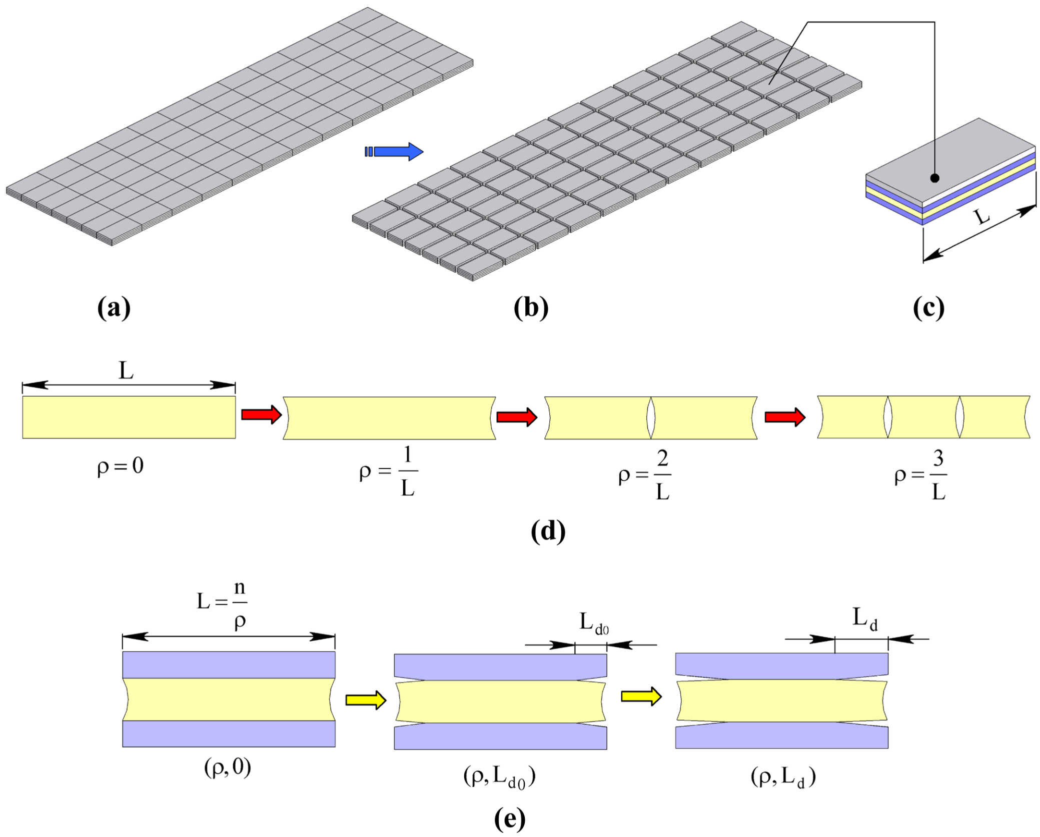

Fig. 1 (a) Typical FE mesh of a general laminate (meso model), (b) elements decomposition, (c) an extracted typical element, (d) matrix crack evolution from the boundary of element, (e) induced delamination growth from the tips of matrix cracks

1- Definition of remote stresses in each selected unit cell (the element dimension should be used as the initial unit cell).
2- Assuming a virtual traverse crack ($\rho = 1/L, 2/L, \ldots$ pattern) in unit cell and evaluating the secondary stress distributions due to considered matrix crack density.
3- Calculating the strain energy release rate due to assumed matrix crack using the obtained stress relations for cracked unit cell in micromechanics model.
4- Checking the possibility of virtual matrix crack growth ($G_m > G_{mc}$).
5- Evaluating the damage parameters and stiffness reduction if the virtual matrix crack happens.

The obtained stiffness reduction due to matrix crack formation should be applied to predict damage formation in meso model.

To consider the delamination growth in a unit-cell with matrix crack, the above-explained stages of 1 to 5 can be used with slight differences. The prerequisite for examining the induced delamination initiation is the existence of matrix crack in unit cell. Then, the calculation steps of damage evolution are:

1- Definition of remote stresses in each selected unit cell.
2- Assuming a virtual delamination length ($L_{d0}, L_d, \ldots$ pattern) in unit cell with specific crack

density and evaluating the secondary stress distributions due to considered delamination length.

3- Calculating the strain energy release rate due to considered delamination length using the obtained stress relations for damaged unit cell in micromechanics model.

4- Checking the growth possibility of virtual delamination ($G_d > G_{dc}$).

5- Evaluating the damage parameters and stiffness reduction if the delamination happens.

It is worth to note that for evaluating the energy release rate of each elements due to transverse cracking formation/delamination propagation, a virtual damage mode (matrix cracking/ induced delamination) is considered in each ply and the secondary stress distribution and energy release rate can be evaluated using the michromechanics approach. After checking the possibility of matrix cracking and induced delamination formations in an arbitrary unit cell, if the criteria for both damage mode formations are satisfied according to step 4, the one with larger strain energy release value is considered in that step. Then the material properties of ply in the element are degraded using relations of (3) which are benefited from micromechanics approach. This degradation is happened according to the assumed virtual matrix cracking density (ρ) or delamination length (δ). These steps are repeated at any specified load step for each element and whole laminate. Following that, the residual forces are calculated for the entire laminate to satisfy the convergence criteria. It is worth to mention that a strength criterion in fiber direction was also used in the code to consider the fiber breakage mode and its effect on the stiffness reduction has also been taken into account. The flowchart of the explained progressive damage analysis in the FE code is available in Fig. 2.

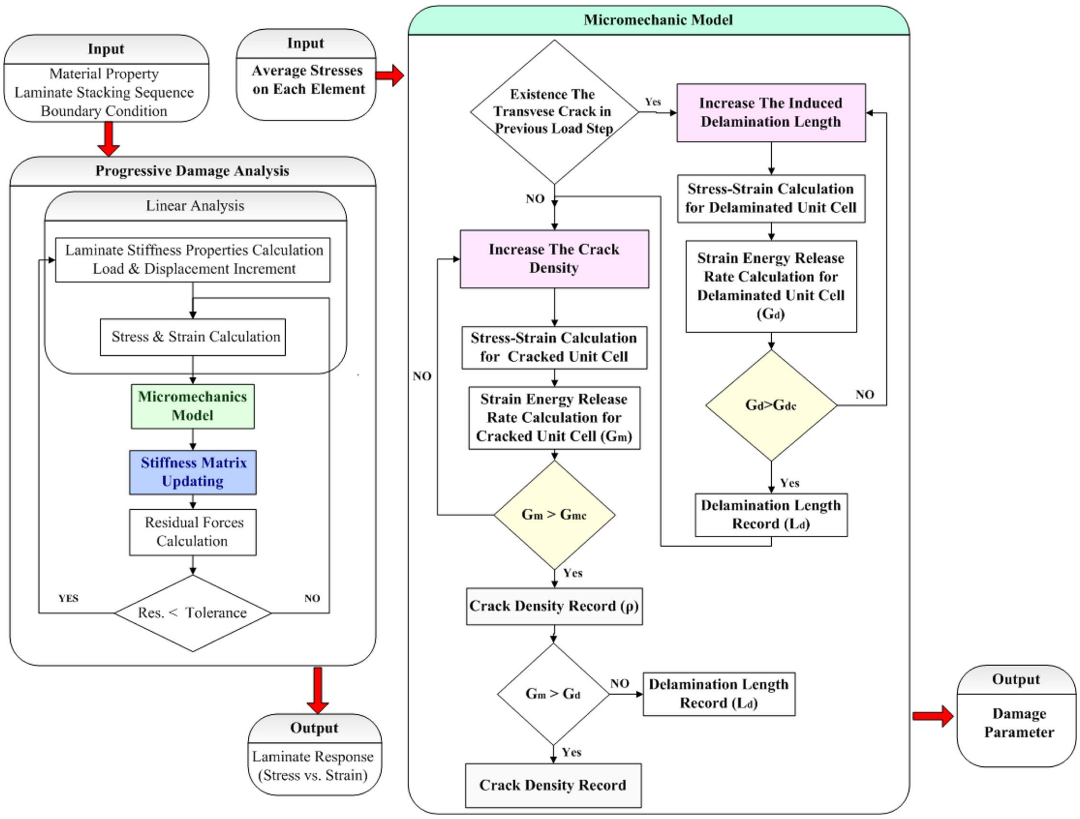

Fig. 2 Flow chart of progressive damage analysis in Micro-meso CDM finite element code

7. Results and discussion

In this section, three different symmetric angle-ply laminates that potentially are subjected to free edge effects are analyzed. The obtained results from the developed micro-meso approach are compared with the obtained results from previously developed traditional CDM (Mohammadi *et al*. 2008). It is worth to mention that the precision and accuracy of the obtained stress distribution in single layer on the basis of developed micromechanical model was examined with the available FEM results for matrix cracking in (Farrokhabadi *et al*. 2010). Furthermore, the calculated energy release rates for matrix cracking and delamination at the specific crack densities were compared with the available results in the literature and/or performed finite element results by the authors to validate the developed micromechanics model (Farrokhabadi *et al*. 2011). Fig. 3 shows the geometry and boundary conditions for a symmetric angle-ply laminate tensile test specimen. Three different angle-ply layups of $[10/-10]_{2s}$, $[30/-30]_{2s}$ and $[45/-45]_{2s}$ are considered. A uniform axial displacement is imposed to specimens at the end $x = L$, while the axial displacement is constrained at $x = -L$. The imposed axial displacement is increased in a series of non-uniform load steps. Also, Fig. 3 shows the 2D finite element mesh using an 8-node quadratic element to model the specimens. The mesh consists of uniform distribution of ten elements along the length of the specimen; however, the refinement level is purposely varied across the width of the specimens. This non-uniform mesh is chosen to permit the free edge interlaminar stresses to be resolved along the lateral edge at $y = W$ and $y = -W$. The selected 2D mesh is according to the suggested criteria in the literature (Mohammadi *et al*. 2008). The size of elements varies across the width of specimens from $y = -W$ to $y = W$ by the order of $t_L/2$, $t_L/2$, t_L, t_L, t_L, $10 \times t_L$, $11 \times t_L$, $50 \times t_L$, $100 \times t_L$, $100 \times t_L$, $50 \times t_L$, $11 \times t_L$, $10 \times t_L$, t_L, t_L, t_L, $t_L/2$ and $t_L/2$ where t_L is the material layer thickness of the laminate. The 2D finite element mesh is shown in Fig. 3(b) and the discretizations through the laminate thickness are also explained in the same figure. The number of divisions along the

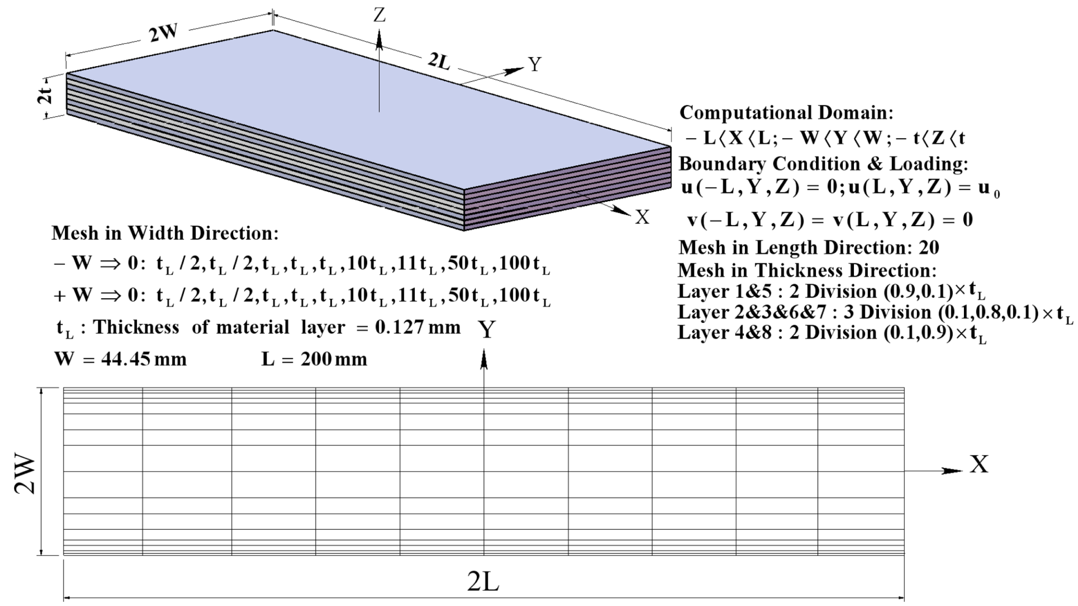

Fig. 3 Through the thickness discretization and plane FEM meshes for a typical laminate

thickness was limited to 20 due to the required large CPU time. The elastic constants for the considered T300/5208 material are E_{11} = 137.11 GPa, E_{22} = E_{33} = 9.58 GPa, ν_{12} = ν_{13} = ν_{23} = 0.28 and G_{12} = G_{13} = G_{23} = 4.48 GPa (Mohammadi *et al*. 2008). The finite fracture toughness of T300/5208 lamina is also G_c = 400 J/m^2 (Farrokhabadi *et al*. 2010).

7.1 Stress-strain behaviors

The resulting stress-strain behaviors for $[10/-10]_{2s}$ angle ply laminates are shown in Fig. 4. This figure shows a good agreement between the obtained results from the present study and experiments (Herakovich 1998) up to the final failure load. It can be observed that for this laminate the response is nearly linear up to the failure load. However, the differences between the results of previously developed CDM in (Mohammadi *et al*. 2008) and present study and experiment could be due to the ignorance of closure effects in (Mohammadi *et al*. 2008). The closure effect on stiffness reduction is not significant in the loading direction of laminate. The resulting stress-strain behaviors for $[30/-30]_{2s}$ angle ply laminate are shown in Fig. 5. This figure also shows a good agreement between the results of the present study and experiments (Herakovich 1998). However, the differences between the results of the previously developed CDM in (Mohammadi *et al*. 2008) and the present study and experiment could be again due to the neglect of closure effects in (Mohammadi *et al*. 2008). Fig. 6 also shows that considering the elastic-damage condition in the analyses induces significant nonlinear behavior on the average axial stress versus axial strain for the layup of $[45/-45]_{2s}$. The obtained results are almost in good agreement with the experimental results and show slightly lower stiffness reduction than the experimental results (over estimate prediction). This figure also shows that, there are not significant differences between the predicted stress-strain behaviors by the present study and CDM (Mohammadi *et al*. 2008) for this laminate. This similarity may be due to the absence of closure effects in this layup.

The predicted stress-strain behaviors up to experimental failure points of $[30/-30]_{2s}$ and $[45/-45]_{2s}$ laminates state that damage parameters may be significantly increased by even a small increment value of the stress. This behavior is similar to ductile conditions. However, the predicted stress

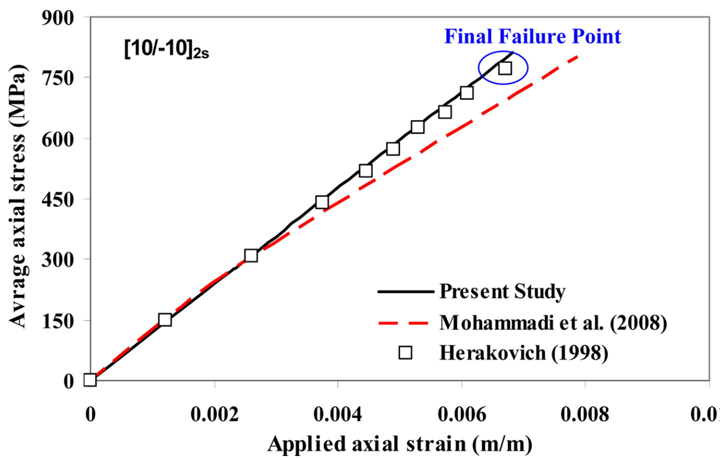

Fig. 4 Average axial stress versus average strain predicted by present study, CDM (Mohammadi *et al*. 2008) and experiments (Herakovich 1998) for $[10/-10]_{2s}$ layup

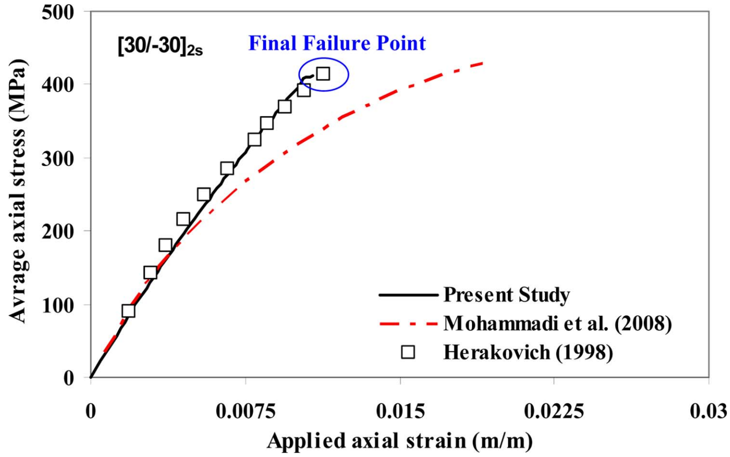

Fig. 5 Average axial stress versus average strain predicted by present study, CDM (Mohammadi *et al*. 2008) and experiments (Herakovich 1998) for $[30/-30]_{2s}$ layup

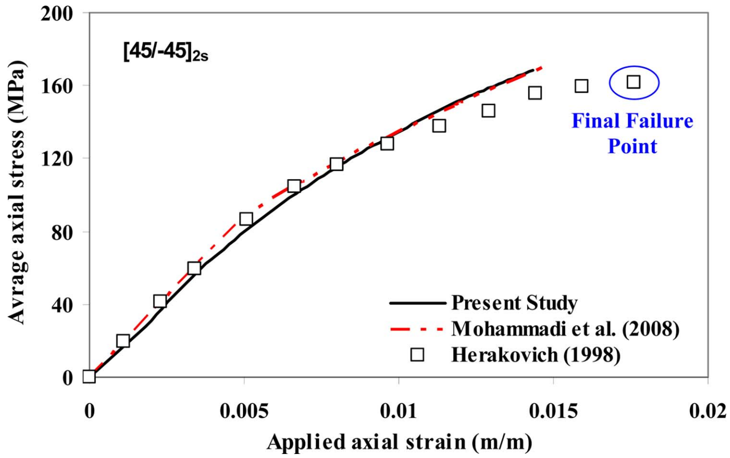

Fig. 6 Average axial stress versus average strain predicted by present study, CDM (Mohammadi *et al*. 2008) and experiments (Herakovich 1998) for $[45/-45]_{2s}$ layup

versus strain for $[10/-10]_{2s}$ laminate shows that its' behavior is similar to brittle conditions. It is worth to note that, the induced delamination fracture toughness, G_{dc}, is assumed equal to matrix crack fracture toughness, G_{mc}.

7.2 Free Edge responses

In this section, the obtained stress distributions near the free edges of various laminates from the present study are compared with those predicted by the previous traditional CDM approach. Fig. 7 shows a good agreement between the obtained through the thickness stresses of σ_{xx}, σ_{yy}, τ_{xy} and τ_{xz} from the present study with those available from CDM (Mohammadi *et al*. 2008) for both elastic-damage and elastic analyses for the layup of $[10/-10]_{2s}$ near the free edges and at the applied load of experimental failure stress of 770 MPa (Herakovich 1998). The minor discrepancy between the

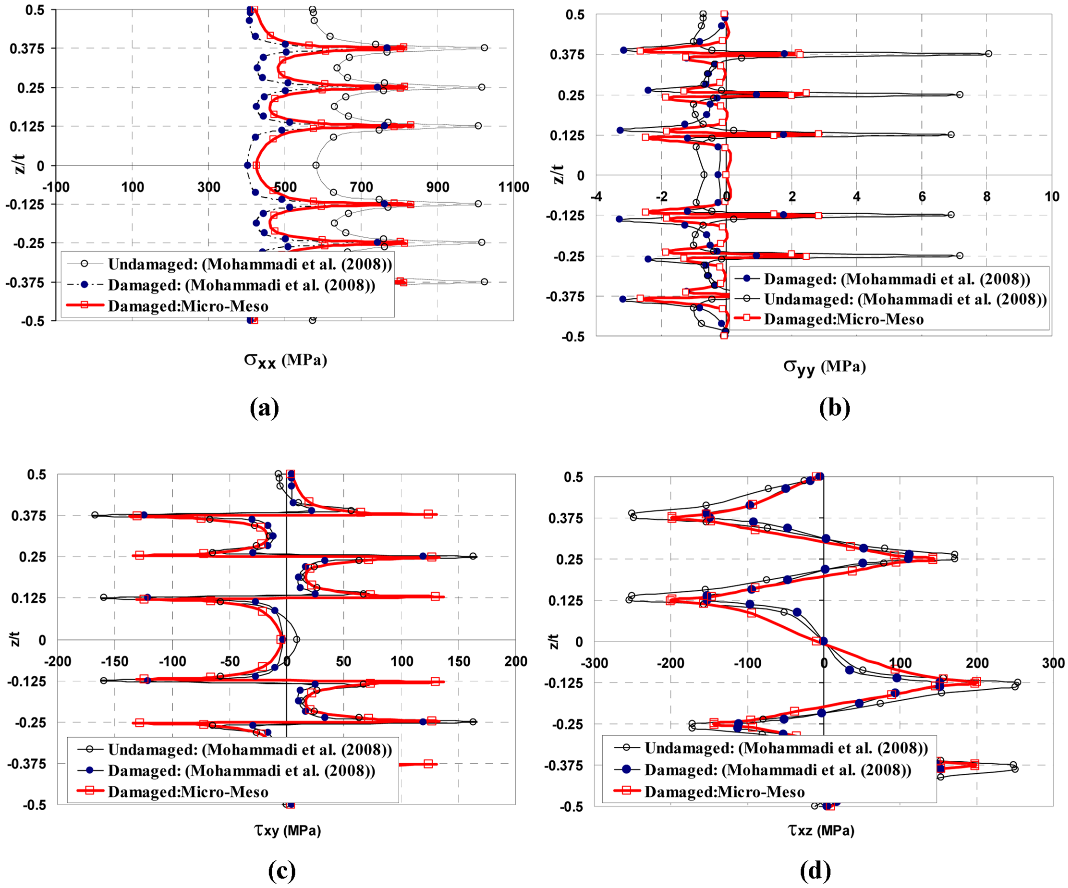

Fig. 7 Variations of stress components through the laminate thickness near free edges for $[10/-10]_{2s}$ layup obtained from present study and CDM (Mohammadi *et al*. 2008), (a): σ_{xx}, (b): σ_{yy}, (c): τ_{xy}, (d): τ_{xz}

obtained results of two studies in elastic analysis could be due to the differences in selection of number of divisions through the thickness and number of elements. This figure also shows that the values of stresses become significantly large at the interfaces of dissimilar plies.

Fig. 7(a) shows that the calculated values of σ_{xx} from elastic-damage analysis are significantly smaller than those obtained for elastic analysis. The values of through the thickness stress of σ_{yy} are negligible for both analyses as observed in Fig. 7(b). There are not significant differences between the values of τ_{xy} from elastic-damage and elastic conditions as shown in Fig. 7(c). Similar to the previous CDM approach, the obtained maximum values of τ_{xz} at the interface of plies with dissimilar angles for damaged condition are partly smaller than those obtained from elastic condition. Although, differences of the obtained distribution of τ_{yz} by the two CDM approaches are not significant, the values of this stress component are small in comparison with the other stress components such as σ_{xx} and τ_{xz} for this laminate.

Fig. 8 compare the variations of obtained stress components near the free edges for $[30/-30]_{2s}$ layup from the present study and CDM in (Mohammadi *et al*. 2008). This figure shows an acceptable agreement between the obtained through the thickness stresses of σ_{xx}, σ_{yy}, τ_{xy} and τ_{xz} from

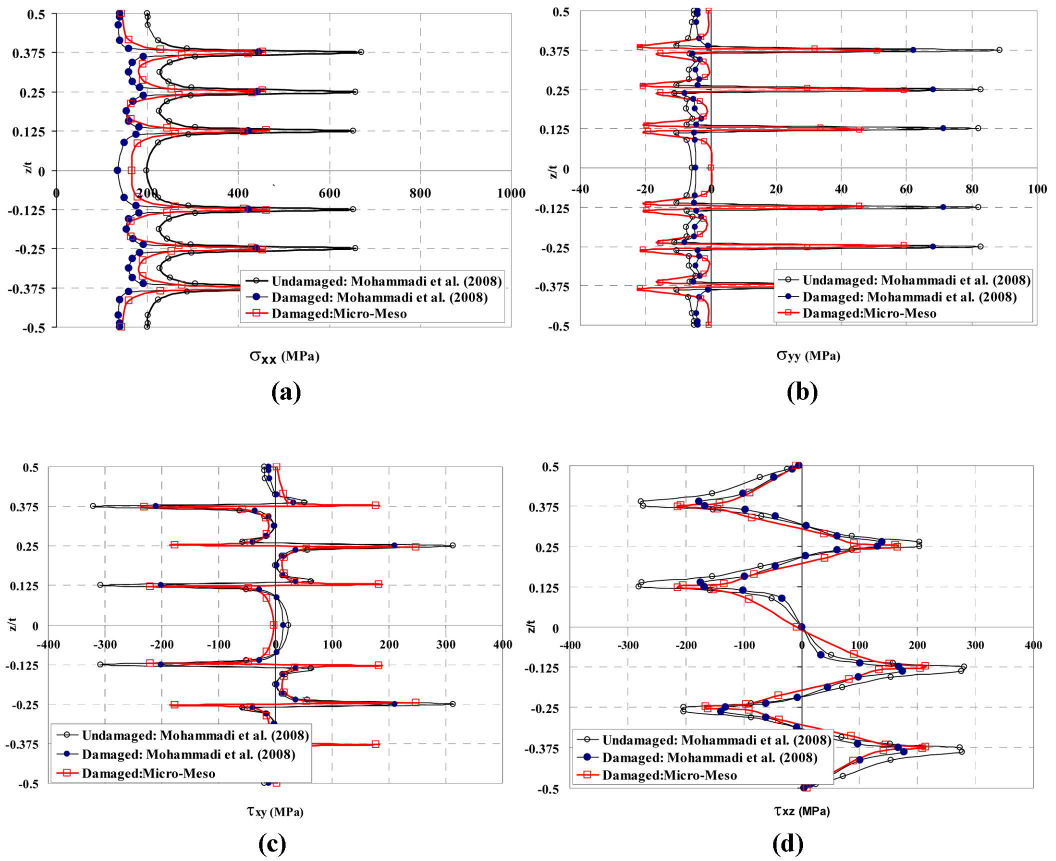

Fig. 8 Variations of stress components through the laminate thickness near free edges for $[30/{-30}]_{2s}$ layup obtained from present study and CDM (Mohammadi *et al*. 2008), (a): σ_{xx}, (b): σ_{yy}, (c): τ_{xy}, (d): τ_{xz}

the present study with those from (Mohammadi *et al*. 2008) for both elastic-damage and elastic analyses at the applied experimental failure stress (410 MPa (Herakovich 1998)).

For this laminate, one reason for minor discrepancy between the obtained results of two studies in elastic part of the analysis can be due to the use of different number of divisions through the laminate thickness and number of elements. Fig. 8(a) shows that the obtained values of σ_{xx} for elastic-damage analysis are significantly smaller than those obtained for elastic analysis. The values of σ_{yy} and τ_{yz} through the laminate thickness are negligible for both analyses as shown in Fig. 8(b) and Fig. 8(e). There are not significant differences between the obtained values of τ_{xy} and τ_{xz} for elastic-damage and elastic analyses as shown in Fig. 8(c) and Fig. 8(d). Similar to the previous CDM approach, the maximum values of τ_{xz} at the interface of plies with dissimilar orientations for damaged condition are partly smaller than those obtained from elastic condition analysis. Although, the differences of τ_{yz} by the two CDM approaches are not significant, and the values of this stress component are small when compared with the other stress components for this laminate.

Fig. 9 show the variations of damage parameters, d' and d'' along the laminate thickness near the free edges for $[10/{-10}]_{2s}$ layup. It is observed that at final failure load of the laminate, the value of d' damage parameter showing in-plane shear modulus reduction is maximum at top and bottom

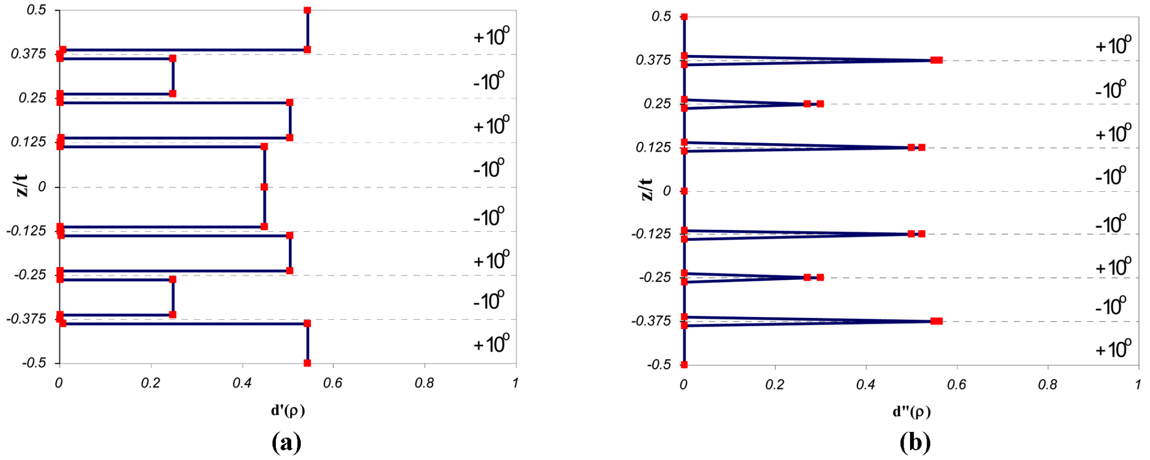

Fig. 9 Variation of damage parameters through the laminate thickness near free edges for $[10/-10]_{2s}$ layup obtained from present study (a) d' and (b) d''

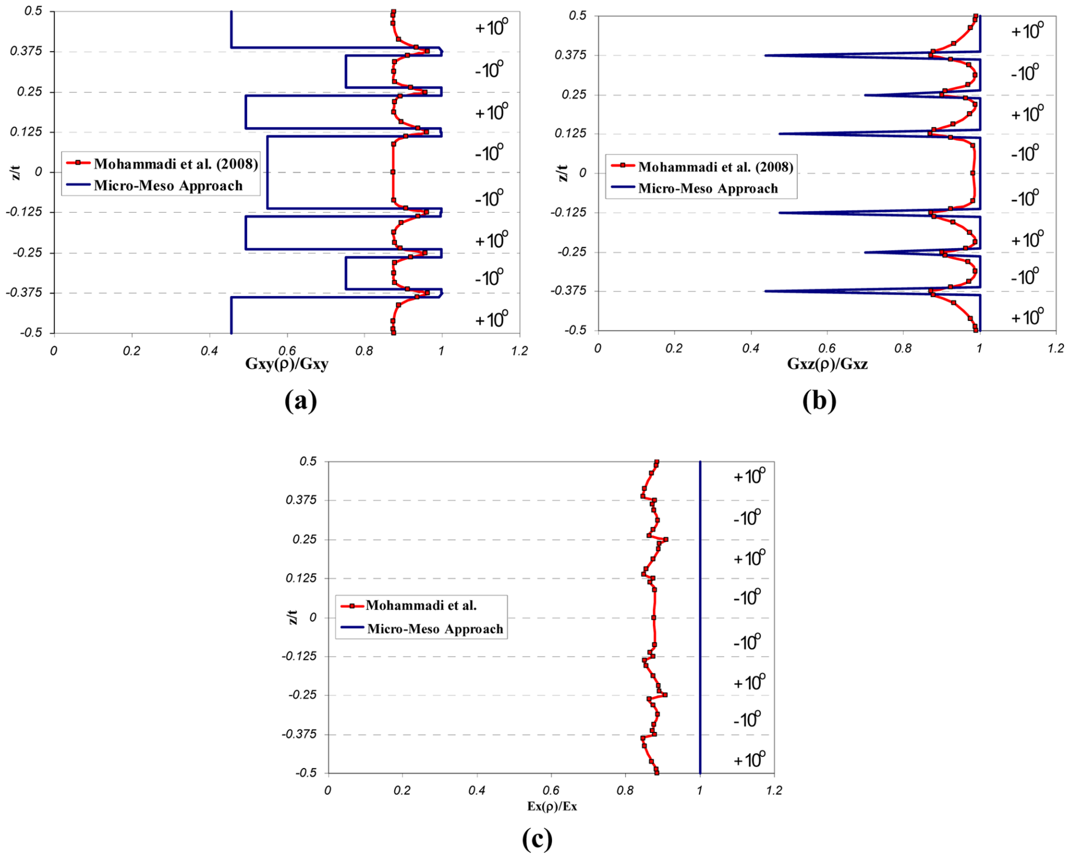

Fig. 10 The ratio of shear modulus through laminate thickness near free edges for $[10/-10]_{2s}$ layup obtained from present study and CDM (Mohammadi *et al*. 2008), (a) G_{xy}, (b) G_{xz}, and (c) E_x

layers of +10º by the value of 0.55 (Fig. 9(a)) and the minimum value of 0.25 occurred at the second top and bottom layers of −10º. The *d″* damage parameter related to delamination growth is maximum with the value of 0.58 at the interface of 10/−10. Fig. 10 shows comparison of normalized shear modulus through the laminate thickness near the free edges for $[10/-10]_{2s}$ layup, which obtained from the present study and Mohammadi *et al*. (2008). It shows that the predicted values of shear modulus reduction by present study are larger than those calculated in Mohammadi *et al*. (2008) for both G_{xy} and G_{xz} components. While the maximum predicted G_{xy} reduction by present study is the ratio of 0.45 in the layer of 10º, the previous CDM approach (Mohammadi *et al*. 2008) predicted the quantity about 0.85 (Fig. 10(a)). For the shear modulus of G_{xz}, while the predicted maximum reduction by micro-meso approach is about 0.45 in the layer of [10/−10], the previous CDM approach predicted the value of this property ratio about 0.85 at the interfaces (Fig. 10(b)). One of the major preferences of present approach when compared to the previous CDM approach (Mohammadi *et al*. 2008) is consideration of the closure effects in the laminates analysis. This capability leads to the prediction of axial elastic modulus reduction of laminate as shown in Fig. 10(c). Fig. 11 shows the predicted variations of *d′* and *d″* damage parameters through the laminate thickness near the free edges for $[30/-30]_{2s}$ layup. It indicates that at experimental failure load of this laminate, the value of *d′* damage parameter (in-plane shear modulus reduction) becomes maximum at top and bottom layer of +30º with magnitude of 0.65 and at the second top and bottom layer of −30º is minimum by the value of 0.30. The *d″* damage parameter value that is proportional to delamination growth has the maximum value of 0.68 at the interface of [30/−30]. Fig. 12 shows a comparison between the ratios of shear modulus through the laminate thickness near the free edges for $[30/-30]_{2s}$ layup obtained from the present study and Mohammadi *et al*. (2008). This figure shows that, for G_{xy} modulus, the predicted reductions by the present study are larger than those by Mohammadi *et al.* (2008). The trend of in-plane modulus variation is also different between two approaches. Contrary to previous CDM approach, in the present study the obtained in-plane shear modulus at the interface is larger than that in through the layer thickness. While the maximum reduction of G_{xy} predicted by present study is about 0.32 in the thickness of 30º ply, the previous CDM approach predicted the maximum value of this material property about 0.80 at the interfaces

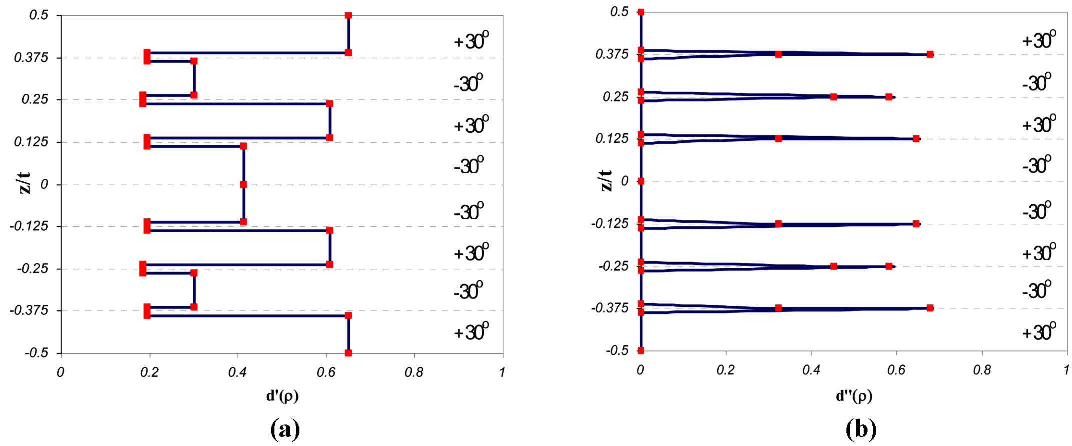

Fig. 11 Variations of damage parameters through laminate thickness near free edges for $[30/-30]_{2s}$ layup, (a) *d′* and (b) *d″*

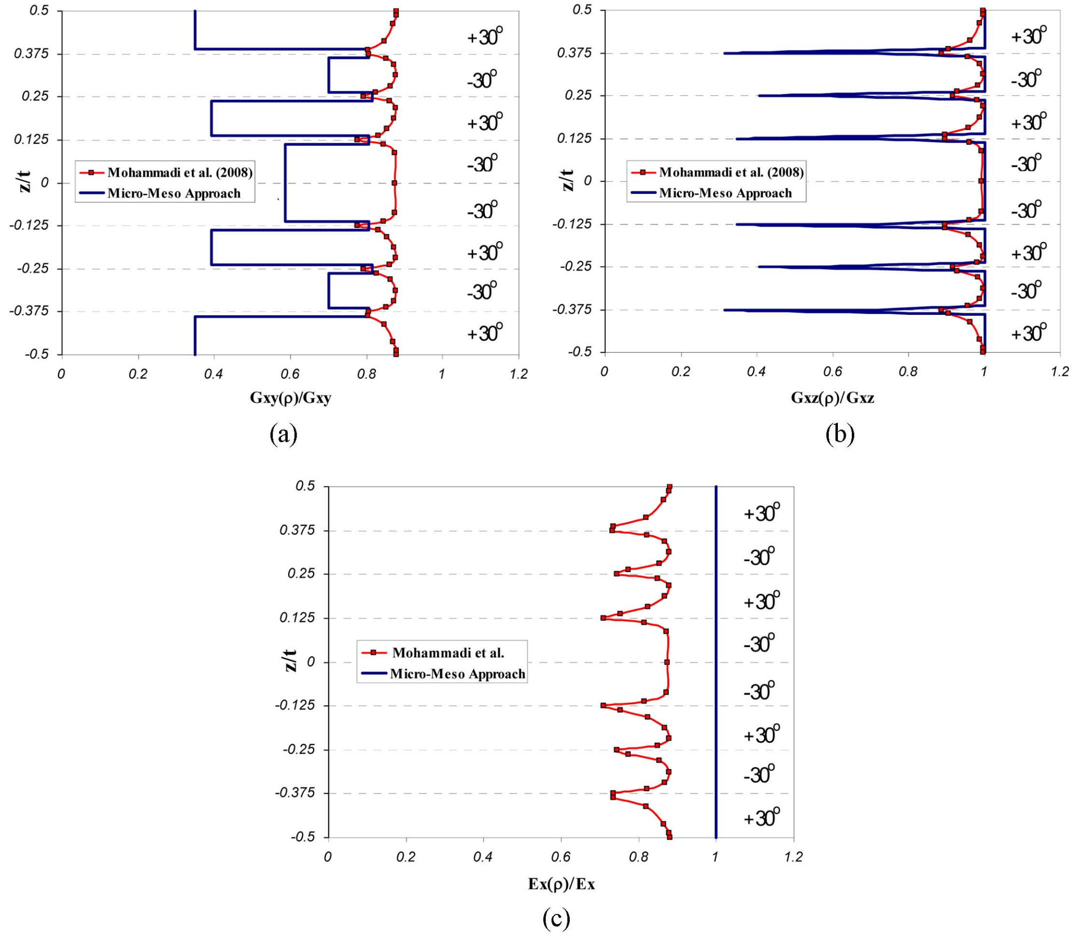

Fig. 12 The ratio of shear modulus through laminate thickness near free edges for $[30/-30]_{2s}$ layup obtained from present study and CDM (Mohammadi *et al*. 2008), (a) G_{xy}, (b) G_{xz}, and (c) E_x

of 30°/−30° plies (Fig. 12(a)). While the maximum reduction of shear modulus, G_{xz}, by present study is about 0.30 in the interface of [30/−30], the value of this material property is about 0.90 in the previous CDM approach. Fig. 12(c) also shows that, at the final failure load, the obtained axial modulus of laminate by two different approaches is dissimilar. This discrepancy is observed in predicted axial stress strain response of this laminate in section 7.1 which is due to nonexistence of closure effects in previous CDM approach (Mohammadi *et al*. 2008). Thus the predicted axial modulus by present approach may be more acceptable. Fig. 13 shows a comparison between the distribution of the $G_{xy}(\rho)/G_{xy}$ and $G_{xz}(\rho)/G_{xz}$ shear modulus ratio through the width of the $[30/-30]_{2s}$ laminate at the $\theta/-\theta$ layer interfaces. The results show that the obtained ratios of $G_{xy}(\rho)/G_{xy}$ by present study are smaller than those from previous CDM approach (Mohammadi *et al*. 2008). While the obtained value of $G_{xy}(\rho)/G_{xy}$ by present study through the width of laminate is about 0.75 (except the points near the free edges, 0.05W), the previous CDM approach reported this value to be about 0.8.

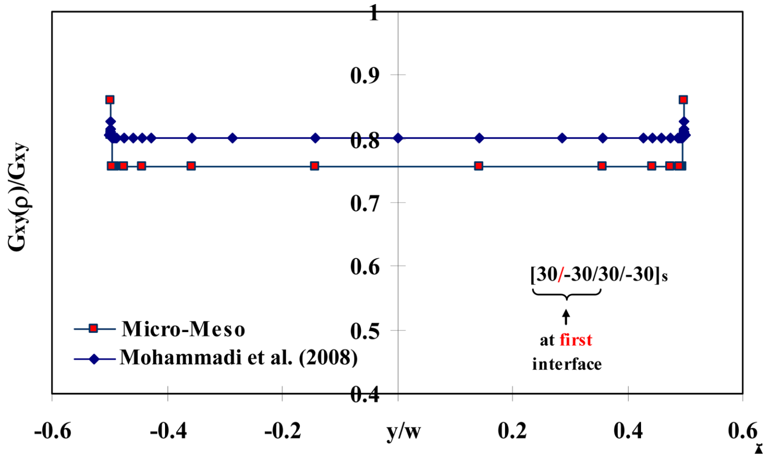

(a)

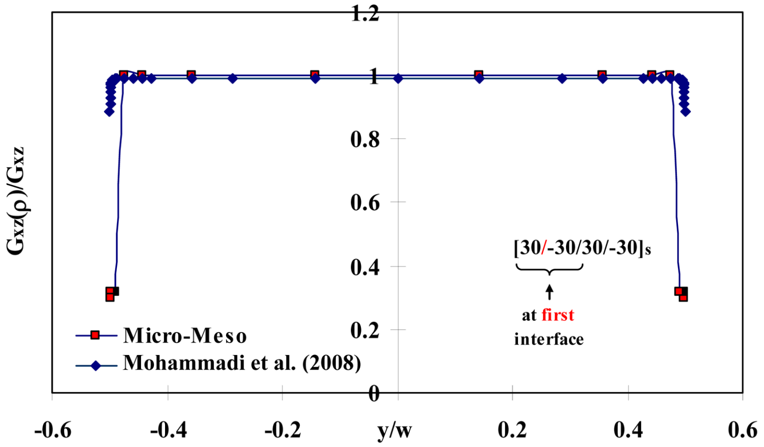

(b)

Fig. 13 The ratio of shear modulus through the width of $[30/-30]_{2s}$ laminate at $\theta/-\theta$ interfaces obtained from present study and CDM (Mohammadi *et al*. 2008), (a) G_{xy}, and (b) G_{xz}

Fig. 13(b) also show that while the predicted value of G_{xz} by present study is about 0.3 near the free edge boundaries, the previous CDM approach reported this value about 0.9. Fig. 14 shows comparison between the distribution of $G_{xy}(\rho)/G_{xy}$ and $G_{xz}(\rho)/G_{xz}$ (shear modulus ratios) of the $[30/-30]_{2s}$ laminate at the $-\theta/\theta$ layers interface. Similar to $\theta/-\theta$ interface layer, the obtained results for the ratio of $G_{xy}(\rho)/G_{xy}$ by present study are smaller than the predicted result by previous CDM approach (Mohammadi *et al*. 2008). Also, the obtained values of G_{xz} by present study are smaller than the previous CDM approach near the free edge boundaries. The obtained results for this layup in Fig. 13 and Fig. 14 show that, near the free edge boundaries about 0.05W, the in-plane and out of plane shear modulus variations are due to the free edge effects on damage parameters of d' and d''.

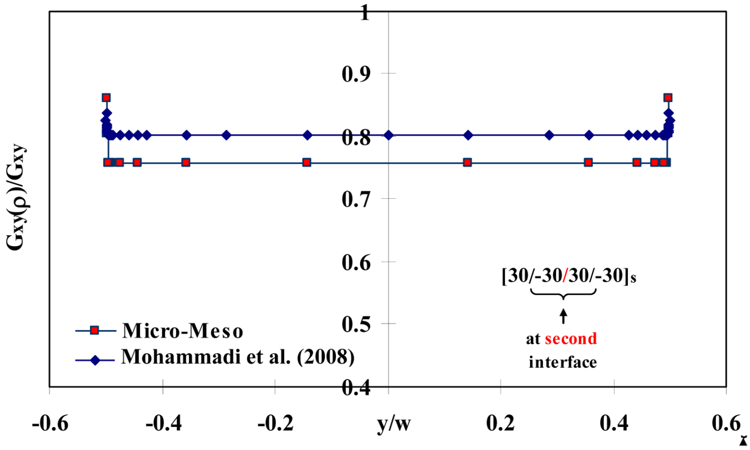

(a)

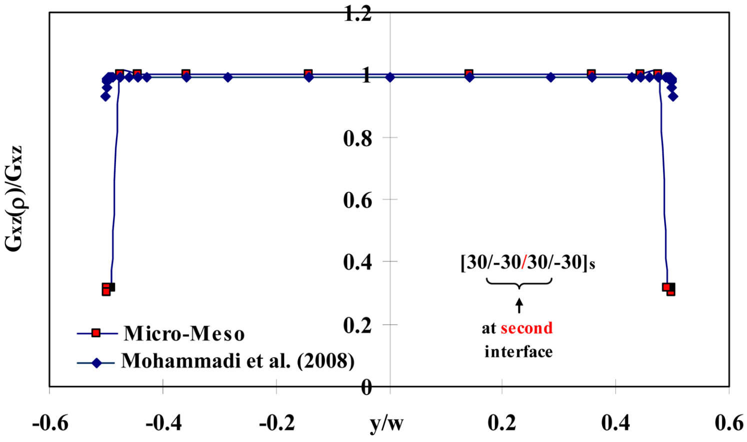

(b)

Fig. 14 The ratio of shear modulus through the width of $[30/-30]_{2s}$ laminate at $-\theta/\theta$ interfaces obtained from present study and CDM (Mohammadi *et al*. 2008), (a) G_{xy}, and (b) G_{xz}

Fig. 15 shows the variation of d' and d'' damage parameters through the laminate thickness near the free edges for $[45/-45]_{2s}$ layup. Fig. 15(a) shows that at failure load of this laminate, damage parameter of d' becomes maximum in the third top and bottom layer of +45º by the value of 0.65 and the second top and bottom layer of –45º has the minimum value of 0.47. According to Fig. 15(b), d' damage parameter which is related to delamination growth has the maximum value of 0.58 at the interface of [–45/45]. Fig. 16 shows comparisons between the ratios of shear modulus through the laminate thickness and near the free edges for $[45/-45]_{2s}$ layup from the present study with those from Mohammadi *et al*. (2008). According to this figure, for $[45/-45]_{2s}$ laminate, the values of shear modulus reduction from present study are larger than those from Mohammadi *et al*. (2008) for G_{xy}. The trend of in-plane modulus variation is also different between the two approaches. Contrary to the previous CDM approach results, the obtained in-plane shear modulus from present study is also larger than those from Mohammadi *et al*. (2008) at different interfaces.

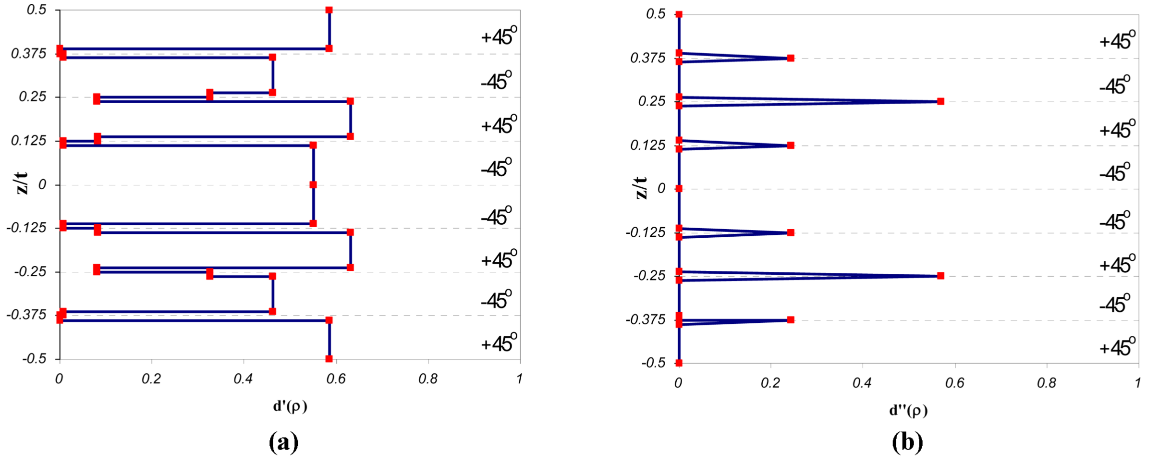

Fig. 15 Variations of damage parameters through the laminate thickness near free edges for $[45/-45]_{2s}$ layup, (a) d', and (b) d''

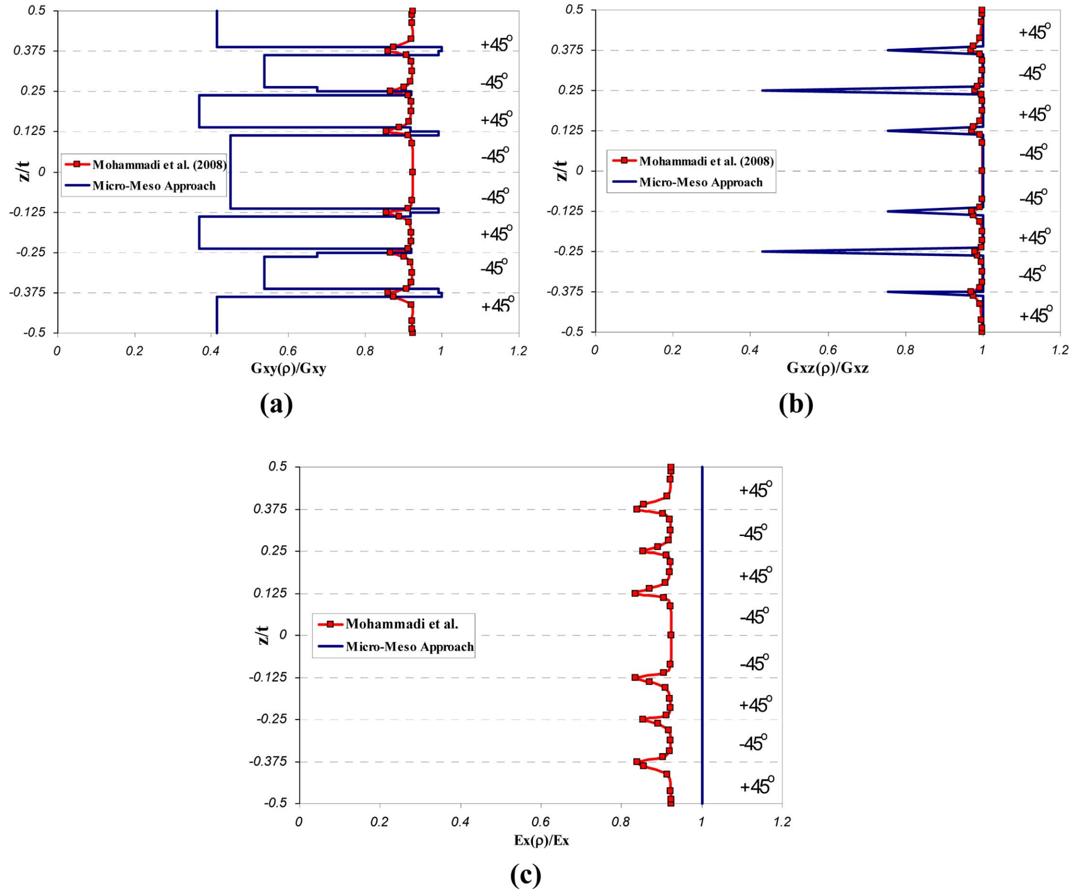

Fig. 16 The ratio of shear modulus through the laminate thickness near free edges for $[45/-45]_{2s}$ layup obtained from present study and CDM (Mohammadi *et al*. 2008), (a) G_{xy}, (b) G_{xz}, and (c) E_x

While the calculated maximum G_{xy} reduction by present study is about 0.35 in the thickness of 45° ply, the previous CDM approach predicted the value of this material property about 0.85 at the 45°/−45° interfaces. For the shear modulus of G_{xz}, while the maximum reduction by present study is about 0.42 in the layer of [45/−45], the previous CDM approach predicted the value of this material property to be about 0.95 at the interfaces.

In general, comparison of the predicted results by present micro-meso approach with different experimental results and previous CDM approach (Mohammadi *et al*. 2008) shown that the predicted progressive damage results by the proposed approach are in an acceptable agreement with the experiments. The predicted overall stress-strain responses for $[10/-10]_{2s}$ and $[30/-30]_{2s}$ laminates by the present approach are in better agreement with the experimental results when compared with those obtained from the previous CDM approach. This is due to the consideration of closure effects in the new proposed micro-meso approach. This capability leads to no reduction in the axial modulus of laminate. The next preference of the newly proposed approach is decreasing the empirical material parameters of damage flow rule that usually have to be obtained from standard and nonstandard experiments. While the present approach needs only one fracture material data (fracture toughness of composite material, G_c), the developed meso-model by ladeveze *et al*. (2000) needs 6 parameters and the required parameters for CDM model presented by mohammadi *et al*. (2008) are about 13 parameters.

6. Conclusions

In this investigation, the recently developed new micro-meso approach by the authors was employed for progressive damage analyses and the edge-effects in various angle-ply laminates and to compare the results with available numerical and experimental results under uni-axial loading. It was shown that the obtained stress-strain behaviors of laminates are in good agreement with the available experimental results and even in better agreement when compared with the results of previous traditional CDM methods. The predicted stress variations and stiffness components through the laminate thickness and near the free edges were also compared with the available CDM results. The main preference of the proposed approach is decreasing the empirical material parameters of damage flow rule that are usually obtained from standard and nonstandard experiments.

References

Abu Al-Rub, R.K. and Voyiadjis, G.Z. (2003), "On the coupling of anisotropic damage and plasticity models for ductile materials", *Int. J. Solids Struct.*, **40**, 2611-2643.

Barbero, E. and De Vivo, L. (2001), "A constitutive model for elastic damage in fiber-reinforced PMC lamina", *Int. J. Damage Mech.*, **10**, 73-93.

Camanho, P.P., Maimi, P. and Davila, C.G. (2007), "Prediction of size effects in notched laminates using continuum damage mechanics", *Comp. Sci. Technol.*, **67**, 2715-2727.

Chaboche, J.L. and Maire, J.F. (2002), "A new micromechanics based CDM model and its application to CMC's", *Aerosp. Sci. Technol.* **6**, 131-145.

Falzon, B.G. and Apruzzese, P. (2011), "Numerical analysis of intralaminar failure mechanisms in composite structures. Part I: FE implementation", *Compos. Struct.*, **93**(2), 1039-1046.

Farrokhabadi, A., Hosseini-Toudeshky, H. and Mohammadi, B., "Development of a damage analysis method in

laminated composites using finite fracture toughness of single lamina", *Mech. Adv. Mater. Struct.* (in press)
Farrokhabadi, A., Hosseini-Toudeshky, H. and Mohammadi, B. (2010), "Damage analysis of laminated composites using a new coupled micro-meso approach", *Fatigue Fract. Eng. Mater. Struct.*, **33**, 420-435.
Farrokhabadi, A., Hosseini-Toudeshky, H. and Mohammadi, B. (2011), "A generalized micromechanical approach for the analysis of transverse crack and induced delamination in composite laminates", *Comput. Struc*., **93**, 443-455.
Hassan, N.M. and Batra, R.C. (2008), "Modeling damage in polymeric composites", *Compos. Part B: Eng*., **39**(1), 66-82.
Herakovich, C.T. (1998), *Mechanics of Fibrous Composites*, John Wiley, New York.
Nguyen, V.T. and Caron, J.F. (2006), "A new finite element for free edge effect analysis in laminated composites", *Comput. Struct.*, **84** (22-23), 1538-1546.
Mishnaevsky, J.R. and Brøndsted, P. (2009), "Micromechanical modeling of damage and fracture of unidirectional fiber reinforced composites: A review", *Comput. Mater. Sci.,* **44**, 1351-1359.
Kant, T. and Swaminathan, K. (2000), "Estimation of transverse/interlaminar stresses in laminated composites / a selective review and survey of current developments", *Compos. Struct.*, **49**, 65-75.
Ladeveze, P., Allix, O., Deu, J.F. and Leveque, D. (2000), "A mesomodel for localization and damage computation in laminates", *Comput. Meth. Appl. Mech. Eng.*, **183**, 105-122.
Ladeveze, P., Lubineau, G. and Marsal, D. (2006), "Towards a bridge between the micro- and mesomechanics of delamination for laminated composites", *Compos. Sci. Technol.*, **66**, 698-712.
Lee, J.W., Allen, D.H. and Harris, C.E. (1989), "Internal state variable approach for predicting stiffness reductions in fibrous laminated composites with matrix cracks", *J. Compos. Mater*., **23**, 1273-1291.
Liu, P.F. and Zheng, J.Y. (2008), "Progressive failure analysis of carbon fiber/epoxy composite laminates using continuum damage mechanics", *Mater. Sci. Eng. A*, **485**, 711-717.
Lonetti, P., Zinno, R., Greco, F. and Barbero, E. (2003), "Interlaminar damage model for polymer matrix composites", *J. Compos. Mater.*, **37**, 1485-1504.
Mohammadi, B., Hosseini-Toudeshky, H. and Sadr-Lahijani, M.H. (2009), "Failure analysis of laminates by implementation of continuum damage mechanics in layer-wise finite element theory", *Struct. Eng. Mech.*, **33**(6), 657-674.
Mohammadi, B., Hosseini-Toudeshky, H. and Sadr-Lahijani, M.H. (2008), "Progressive damage analysis of angle-ply laminates exhibiting free edge effects continuum damage mechanics with layer-wise finite element method", *Fatigue Fract. Eng. Mater. Struct*., **31**, 549-568.
Raghavan, P. and Ghosh, S. (2005), "A continuum damage mechanics model for unidirectional composites undergoing interfacial debonding", *Mech. Mater*., **37**(9), 955-979.
Varna, J. (2008), "Physical interpretation of parameters in synergistic continuum damage mechanics model for laminates", *Compos. Sci. Technol.*, **68**, 2592-2600.
Voyiadjis, G.Z. and Kattan, P.I. (1999), *Advances in Damage Mechanics: Metals and Metal Matrix Composites*, Elsevier, Amsterdam.
Voyiadjis, G.Z. and Park, T. (1999), "Kinematics description of damage for finite strain plasticity", *J. Eng. Sci*., **37**, 803-830.
Voyiadjis, G.Z. and Deliktas, B. (2000), "A coupled anisotropic damage model for the inelastic response of composite materials", *Comput. Meth. Appl. Mech. Eng*., **183**, 159-199.
Voyiadjis, G.Z., Deliktas, B. and Aifantis, E.C. (2001), "Multiscale analysis of multiple damage mechanics coupled with inelastic behavior of composite materials", *J. Eng. Mech.*, **127** (7), 636-645.
William, K.V., Varizi, R. and Poursartip, A. (2003), "A physically based continuum damage mechanics model for thin laminated composite structures", *Int. J. Solids Struct.*, **40**, 2267-2300.